

LATITUDINAL PLASMA DISTRIBUTION IN THE DUSK PLASMASPHERIC BULGE:  
REFILLING PHASE AND QUASI-EQUILIBRIUM STATE

P. M. E. Décréau,<sup>1,2</sup> D. Carpenter,<sup>3</sup> C. R. Chappell,<sup>1</sup> R. H. Comfort,<sup>4</sup>  
J. Green,<sup>1</sup> R. C. Olsen,<sup>4</sup> and J. H. Waite, Jr.<sup>1</sup>

**Abstract.** This paper analyzes the plasma characteristics measured in the dusk sector of the plasmasphere during the period May-June 1982, mainly by the satellites DE 1 and GEOS 2, in order to examine the hypothesis of a lack of connection between the equatorial plasmaspheric bulge and the underlying ionosphere. The orbits of the spacecraft allow a study of the dusk bulge from two different perspectives: GEOS 2, geostationary, yields the local time variations of the plasma parameters, whereas DE 1 stays roughly in a meridian plane and provides their latitudinal variations. Different techniques (waves and ion spectrometer in the very low energy range) are used and compared. A period of a few days (May 22-26) is analyzed in detail. Large density irregularities are commonly observed, as well as significant plasma drifts, but the bulge does not seem to be limited in latitude, at least between +40 and -40 degrees magnetic latitude. The analysis of the plasma distribution along a field line shows the existence of different plasma regimes, depending on the geophysical conditions encountered. In particular, we have observed (1) during the replenishment of depleted flux tubes, an apparent accumulation of plasma at about 3 earth radii and 40° latitude, and a double field-aligned regime in the equatorial region, and (2) under conditions of moderate magnetic activity, the appearance of a high density region, with origin presumably in the inner plasmasphere, extending to geostationary orbit. In this region of  $L = 4.6$  to 6, the density, normalized to the volume of the flux tubes, is constant over the latitudinal range explored (from minus to plus 40°), as expected from a diffusive equilibrium distribution.

1. Introduction

Recently, several investigations of the outer plasmasphere have shown the presence of a region of very low-energy trapped ions, mostly protons, located near the magnetic equator [Horwitz et al., 1981; Olsen et al., 1981; Wrenn et al., 1984]

These ions are commonly observed in a region of moderate density (near  $100 \text{ cm}^{-3}$ ) characteristic of the plasmopause boundary and of the plasmaspheric bulge. The equatorial trapped distribution is believed to be due to wave heating of the main thermal component. The resulting energies are of the order of 10 eV. Due to the presence of this distinctive plasma regime, the density distribution along a field line might be expected to show some irregularity in the vicinity of the equator. Considering that there is no evidence of a dusk bulge at the ionospheric level [Brace and Theis, 1974; Titheridge, 1976], some authors have raised the hypothesis of a lack of connection between the equatorial plasmaspheric bulge and the underlying ionosphere [Chappell, 1982; Reasoner et al., 1983]. Moreover, a temporary confinement of isotropic plasma to the equatorial region is envisioned in the models of Banks et al. [1971] for the refilling of plasmaspheric flux tubes. This scenario is still open to critical questions [Horwitz, 1983] since no experimental evidence of equatorial density enhancement or formation of associated shock fronts has been found. Actually, a field-aligned distribution of thermal ions, with enhanced fluxes in both the northern and southern hemisphere source cone, has been observed on GEOS 1 near the equatorial plasmopause in the morning magnetosphere [Wrenn et al., 1984]. Such distributions are interpreted as a signature of the filling process occurring outside the plasmasphere when flux tubes are relatively empty. The latitudinal extension of those distributions is not known, as only few cases of similar observations have been reported [Horwitz et al., 1981; Sojka et al., 1983].

In this paper we examine the latitudinal structure of the bulge under quasi-steady conditions as well as during the recovery phase. In the former case, we study the properly so called bulge: the region of moderate density formed by the expansion of the main plasmaspheric body on the duskside of the magnetosphere. During the recovery phase, we concentrate on the region of lower density located outside the plasmasphere, and examine the evolution of the plasma regime, showing mainly field-aligned distributions, versus the magnetic latitude. Our study is based on comparisons of plasma measurements made by the GEOS 2 and DE 1 spacecraft during a period of low and moderate magnetic activity. It takes advantage of the peculiarity of the DE 1 orbit, which follows approximately a magnetic field line in the equatorial region during the period studied. After a description of the available data set, including orbital features of the spacecraft and types of measurements (section 2), we present the compared density measurements in different parts of the dusk bulge (section 3). In section 4 we discuss these observations, in particular the

<sup>1</sup>Space Science Laboratory, NASA Marshall Space Flight Center, Huntsville, Alabama.

<sup>2</sup>Permanently at Laboratoire de Physique et Chimie de l'Environnement et Université d'Orléans, Orléans, France.

<sup>3</sup>Space, Telecommunications and Radioscience Laboratory, Stanford, California.

<sup>4</sup>Department of Physics, University of Alabama in Huntsville.

Copyright 1986 by the American Geophysical Union.

Paper number 5A8766.

0148-0227/86/005A-8766\$05.00

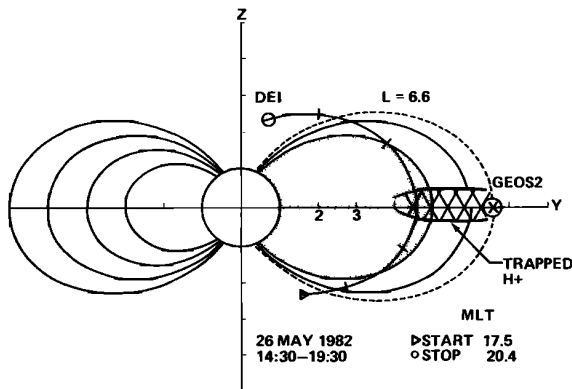


Fig. 1. DE 1 and GEOS 2 orbits in the ZY plane of geomagnetic coordinates, for one DE 1 pass in the period studied. Each point has been rotated in MLT. The shadowed and hatched regions refer respectively to the plasmasphere and trapped proton regions.

result of an attempt to derive a density profile along a field line from measurements made along the DE 1 orbit. Finally, we discuss the hypothesis of an equatorial density enhancement, and summarize the new findings obtained in this exploration of the bulge by two satellites of complementary orbits (section 5).

## 2. Data Base

During the time period chosen for the study (May 22 to 26, 1982), the orbit of DE 1 is almost symmetric with respect to the magnetic equatorial plane (Figure 1), with some variations in the latitude of the apogee ( $\pm 10^\circ$ ) according to the universal time of the pass. The satellite stays in the range 1700–2000 MLT for the high altitude part of its orbit (at a geocentric distance  $R \approx 2.5 R_p$ ). It crosses the L shell of GEOS 2 ( $L = 6.6$ ) near  $45^\circ$  latitude. The operations of the plasma instruments, as well as the data acquisition are almost continuous, as indicated in Figure 2. GEOS 2, which is geostationary, provides the local time variations of the plasma parameters in the equatorial plane. Its operations are reduced to the afternoon and night hours (Figure 2). The corresponding MLT range. (1615–0415) covers the region of the dusk bulge and the night sector of the magnetosphere.

The DE 1 crossings of the GEOS 2 L shell (at times indicated in Figure 2) occur in the dusk sector, but are not at exactly the same MLTs. For each high altitude orbit, DE 1 requires  $\approx 5$  hours to travel between  $L = 6.6$  in one hemisphere and  $L = 6.6$  in the other. Depending on the universal time considered, its MLT variations are either negative or positive during this period. They stay typically within one hour, in the sector (1730–1930) MLT. The corresponding scan in magnetic longitude is always significant, westward and covering a range of  $40^\circ$  to  $90^\circ$ . As a result, GEOS 2 and DE 1 view the plasmaspheric region in a different way: under very quiet conditions, where corotation dominates up to 6.6 L value and above, GEOS 2 more or less follows a given plasma cloud, whereas DE 1 scans a wide segment of plasma and

provides a kind of azimuthally averaged latitudinal profile of the plasma structure. Under disturbed conditions, GEOS 2 will eventually see sunward drifting plasmas in the dusk sector, while DE 1 may stay in a more stagnating region at lower L shells. In addition, there can be an important time lag between the universal times of DE 1 and GEOS 2 measurements on a given field line. Only a few of them may be considered as magnetic field line conjunctions.

The probing of magnetospheric plasmas of very low energy at high altitude, i.e., in a low density environment, is a complicated task. As a consequence of photoemission and spacecraft charging, low-energy particle trajectories are affected in the vicinity of the probe to an extent which is difficult to quantitatively evaluate. The use of active wave techniques [Etcheto and Bloch, 1978; Décréau et al., 1978a], as well as eclipse measurements [Olsen, 1982] has demonstrated the existence of a cold population in the outer plasmasphere, which is sometimes hidden from the particle detectors. This emphasizes the need for understanding charging processes affecting particle analyzers [Olsen et al., 1983; Comfort et al., 1985]. Both wave and particle analyzer techniques will be utilized and compared in this paper.

On GEOS 2, the characteristics of the thermal electrons are measured by natural wave analyzers, a resonance sounder and mutual impedance active instruments [S300 Experimenters, 1979] which operate in turn. These wave techniques yield information on the first moments of the particle distribution function. The density is measured through the identification of the upper hybrid frequency. The temperature, provided by the mutual impedance device, is derived through the determination of the electron Debye length. These measurements are free from the consequences of spacecraft charging [Décréau et al., 1978b] and are reliable in the outer plasmasphere. Also part of the wave experiments is a Dc electric field probe which measures the equatorial plasma drifts

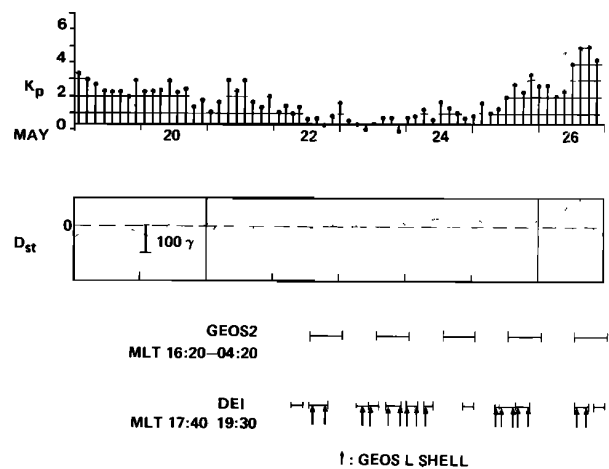


Fig. 2. Times of data acquisition for each satellite and the associated Kp and Dst variations for the period studied. Arrows correspond to times when DE 1 crosses the GEOS 2 L shell.

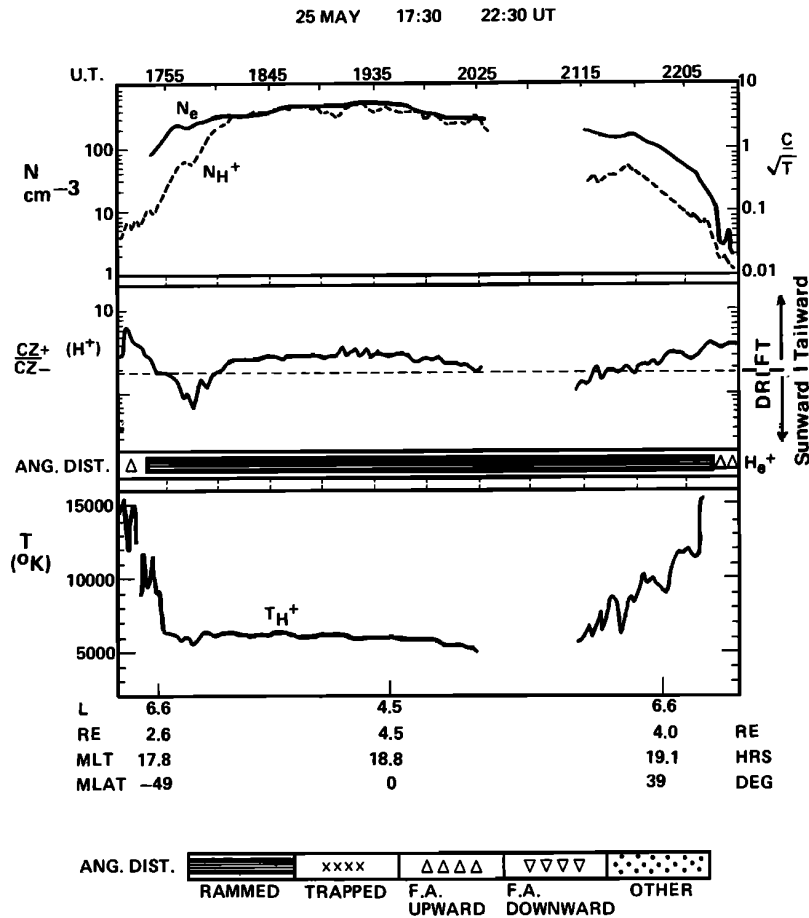


Fig. 3. DE 1 plasma measurements along one pass, derived from the plasma wave instrument (PWI), and from the retarding ion mass spectrometer (RIMS). Electron density, in the top panel, is obtained from the upper hybrid resonance observed by PWI. The proton density is obtained by RIMS, from the ratio of the flux C to the square root of the temperature. The ion drift, which can distort the inferred density and temperature (plotted in the bottom panel), is indicated in the center panel by the ratio of the fluxes in the detectors looking along the spacecraft spin axes, i.e., east-west.

relative to the satellite [Pedersen et al., 1978].

On DE 1, both electron and ion characteristics are examined. The electron density  $N_e$  is provided by the upper hybrid frequency signature when available in the natural wave spectrum measured by the plasma wave instrument (PWI) [Shawhan et al., 1981]. The ion information is given by the retarding ion mass spectrometer (RIMS) instrument [Chappell et al., 1982b], which uses a combination of a retarding potential analyzer (RPA) (0-50 eV) and a magnetic ion mass spectrometer (1-40 amu). The parameters determined during the five-day period were: hydrogen density and temperature (of an assumed isotropic population), helium pitch angle distribution and azimuthal flow velocity.

An example of the DE 1 observations used for this study is presented in Figure 3. The upper panel shows the density variations along the orbit for the electrons and protons (helium and oxygen are minor constituents in the region explored). The proton density,  $N_{H^+}$ , is assumed to

be proportional to the ratio  $C/\sqrt{T}$  between the count rate C measured at zero retarding potential, and the square root of the temperature. This approximation is valid for an isotropic, non drifting ion population, when the satellite potential is negligible (D. Young, unpublished manuscript, 1978). The temperature (see bottom panel) is obtained from a simple calculation of the peak slope of the RPA curve and has been carefully calibrated against a computer algorithm using the thin sheath approximation [Comfort et al., 1982]. The temperature calculation also assumes as negligible both plasma drifts and spacecraft potential. The validity of this assumption is indicated by the region of agreement between PWI and RIMS density measurements. The amplitude of plasma drifts (for protons) along the earth-sun direction is qualitatively indicated in the middle panel by the ratio  $CZ^+/CZ^-$  between the hydrogen counting rates at zero RPA voltage of the two RIMS end heads, aligned with the spin axis, which look respectively toward and away

from the sun. The reference value of this ratio, which has been derived through the measured Dc electric field, corresponds to a zero drift relative to the satellite. When the measured value stays within a factor of 2 from the reference value, estimated drifts for typical temperatures ( $\approx 4000^\circ\text{K}$ ) stay below a few kilometers per second.

Another important piece of information is the angular distribution of the particles. This is provided by the radial head looking perpendicular to the spin axis, and shown qualitatively in the middle panel of Figure 3, in this case for helium. Examples of different angular distributions, as they appear in the measurements, are shown and discussed below (section 4.3). The proton angular distribution is not available in the particular time period May 22-26, 1982, due to temporary degradation of the channeltron detectors. Hydrogen and helium distributions are expected to roughly follow one another in both the isotropic (seen as rammed distribution) or field-aligned regimes. However, trapped distributions of hydrogen and helium are not systematically associated, at least in the equatorial region. The trapped distribution can be further identified by the associated increase of temperature (R. C. Olsen et al., unpublished manuscript, 1984), which is measured by the end heads.

It appears from Figure 3 that the plasma parameters measured near the GEOS 2 field line ( $L = 6.6$ ) are obtained in a transition region. This is indicated by (1) the proximity of the boundary between isotropic and field-aligned distributions, (2) enhancements of the temperature relative to measurements made at lower L shells, and (3) discrepancies between  $N_e$  and  $N_{H^+}$ . This last clue indicates the existence of a cold population which becomes hidden, presumably due to the positive charge of the satellite, when the density decreases below a certain level. We have compared  $N_e$  and  $N_{H^+}$  measurements during the several days of our study, at times when DE crosses the equator (near  $L = 4.6$ ) and the 6.6 L shell respectively, and when the  $N_{H^+}$  calculation is significant. The same behavior is observed systematically: there is good agreement between both measurements at the equator, where densities are higher than  $100 \text{ cm}^{-3}$ , and disagreement, with a factor of 2 to 10, on the GEOS L shell when lower densities and higher spacecraft potentials exist. Consequently, for the quantitative comparisons between both spacecraft, we will use  $N_e$  values. RIMS data at  $L = 6.6$  are still useful, as they provide the characteristics of the particle distributions, in angle and energy, in the suprathermal range.

In addition to the GEOS 2 and DE 1 data, we have used  $N_e$  measurements from two other sources: whistler data recorded on the ground at the Antarctic station Siple and the resonance sounder instrument on board ISEE 1 (Harvey et al., 1978). These sources provide the radial density distribution in the dusk sector, at or near the equator, in the inner ( $L < 5$ ) and outer plasmasphere, respectively.

### 3. Observations of the Morphology and Dynamics of the Bulge

Density profiles along the orbit of GEOS 2 (Figure 4) give an idea of the dynamics of the

equatorial convection pattern and plasmasphere refilling during the period under study. The profiles are presented in polar coordinates, where the radial scale is linear versus the plasma frequency. During the first two passes, the density stays low and shows only slight azimuthal variations. The density measured at 1800 MLT on orbit A ( $N_e = 5.8 \text{ cm}^{-3}$ ) corresponds to the density expected in a flux tube initially empty in the night sector of the magnetosphere, after its drift once around the Earth, assuming an upward flux of  $3 \times 10$  electrons  $\text{cm}^{-2} \text{ s}^{-1}$  [Park, 1970], and a drift time of roughly 18 hours. Experimental support for this figure is provided by density profiles measured on GEOS 2 during earlier continuous operations. These profiles show an increasing density versus MLT on the dayside, which is approximately  $4 \text{ cm}^{-3}$  per 12 hours when corotation dominates [Décréau, 1983].

On May 22, GEOS 2 is located just radially outside of a clear plasmopause gradient which is identified at  $L = 6.1$  on the radial density profile measured by ISEE 1, approximately 3 hours later. Because of the presence of cold plasma in the dusk and night sector, one may consider that a second plasmopause, in the process of formation, is located outside of the geostationary orbit. In the night (May 22-23) however, an isolated increase of the Kp index took place (Figure 2), associated with an increase of the convection electric field in the midnight sector, as revealed by the density decrease at the end of the orbit A profile (Figure 4). As a consequence, the density measured on the next orbit by GEOS 2 is interpreted as again representative of the first stage (less than 24 hours) of ionospheric refilling. The plasmopause boundary is presumably not far inside of GEOS 2.

The next day (orbit C), the satellite crosses the plasmaspheric bulge in the late afternoon. The higher densities ( $N_e \approx 50 \text{ cm}^{-3}$ ) measured near 2000 MLT cannot be explained by a two-day refilling process, at least not according to the figure of an increase of density  $N_e$  of  $8 \text{ cm}^{-3}$  per day. They are likely due to a movement of the inner plasmasphere in the dynamics of the convection pattern. A dusk bulge is still visible in the next two orbits (D and E). The strong density fluctuations observed probably reflect the variability of the convection electric field, associated with the increase of magnetic activity on May 25. The electric field measured on board the satellite in the dusk sector is negligible up to May 26, but earlier spatial and temporal variations, not necessarily visible to GEOS 2, could have imposed structure upon the plasma. The ISEE 1 radial density profile from May 25 is irregular also.

The DE 1 electron densities measured during the same period are shown in Figure 5. The plots are presented as a function of UT, centered around the equator crossing. The letter G refers to the times when DE 1 crosses the GEOS 2 L shell. On the first two days (May 22-23), when GEOS 2 sees no irregularities, the meridian profiles show strong density variations. As stated above, GEOS 2 sits just outside of the outer edge of the plasmopause. Due to the very low activity, the plasma may approximately corotate at synchronous orbit with the spacecraft, and show only slow variations of the plasma parameters. DE1 reaches lower L shells,

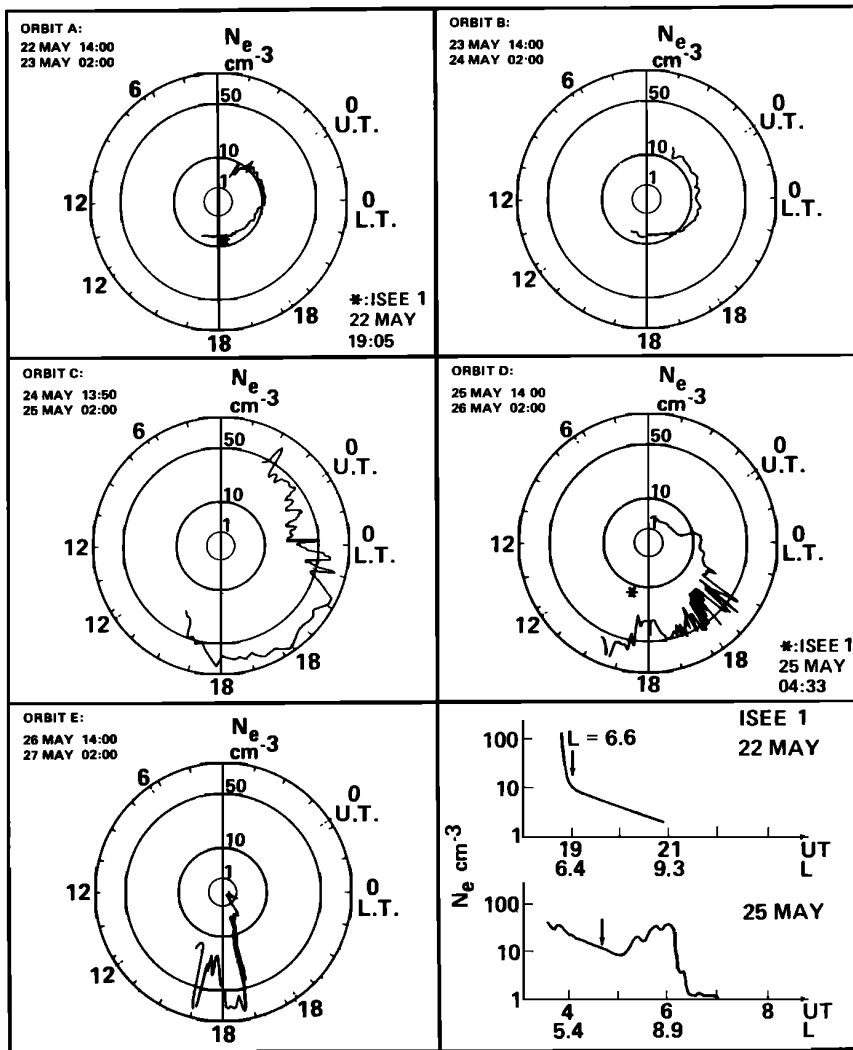


Fig. 4. Polar plots of electron densities measured on GEOS 2. The radial scale is linear in plasma frequency. The asterisks refer to densities measured by ISEE 1 near the equator, for  $L = 6.6$ . All times indicated are UT in hours and minutes.

through a region of density gradient which may have been structured earlier during disturbed conditions. The plasma structures, moving in approximate corotation, are scanned by the satellite and shown in the measured profiles.

A strong asymmetry between the two hemispheres appears in the last May 23 profile (1948 UT). This feature, which is seen with more detail by the RIMS instrument, will be discussed in section 4. On the next two days (May 24-25), the density distribution reported by DE 1 appears to have reached an equilibrium along the flux tubes: the profiles are smooth, at least below  $L = 6$ . The region of density irregularities seen in the GEOS 2 azimuthal profile of May 25 (Figure 4) has presumably moved to higher L shells than for the first two days. Also, although the electric field measured on GEOS 2 is still below the sensitivity of the instrument ( $\approx 1 \text{ mV m}^{-1}$ ), a westward component of the convection may be at work in the bulge, which slightly reduces the scanning effect at DE. The last profile shown in Figure 5 is taken during a disturbed period (see Kp and Dst variations in Figure 2). GEOS 2 profiles at the time of orbit E also show large

density variations which we interpret as being mostly due to irregular plasma drifts, which are measured at that time on GEOS 2 and DE 1.

Direct comparisons between GEOS 2 and DE 1 densities measured at  $L = 6.6$  are shown in Figure 6. On the same graph, we present the density variations seen by DE 1 at the equator ( $L \approx 4.6$ ). The equatorial values reported increase progressively during the refilling period (May 22-23), after which they stay in the range of  $200\text{-}400 \text{ cm}^{-3}$  during what we will call the expanded bulge period (up to May 26). At  $L = 6.6$ , the refilling period is characterized by a large discrepancy between GEOS 2 and DE 1 latitude values. At DE 1 latitude ( $\pm 45^\circ$ ), either the density values reported are much larger than measured at the equator by GEOS 2, or no upper hybrid frequency signature is observed. In the latter case, that is, for those times indicated at the bottom of Figure 6, the density is probably low, as is also suggested by RIMS. A consistent discrepancy between densities measured at low latitude (by GEOS) and at middle latitude (by DE) could be simply predicted in a collisionless model of the plasma distribution on

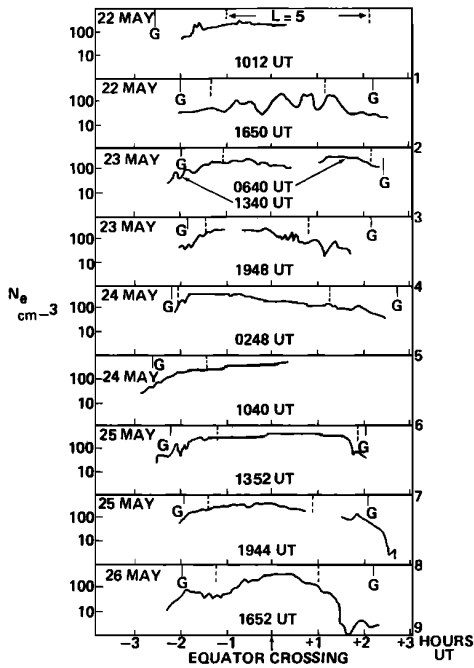


Fig. 5. Electron density versus time profiles for successive passes of DE 1. The plots are centered at the time of the equator crossing. The G letters and vertical dashed lines refer to crossings of the 6.6 and 5 L shells respectively.

a given field line, which approaches a distribution  $N_e \propto R^{-4}$  [Angerami and Carpenter, 1966; Lemaire and Sherer, 1974; Corcuff and Corcuff, 1982]. However, the presence of low densities at DE latitudes, observed in between higher-density measurements, and not systematically related to a given hemisphere nor to the highest altitudes, are in favor of an explanation based on the presence of plasma structures.

The May 24-25 period is characterized by a reasonable agreement between densities taken in different locations of the bulge. At the equator, the  $L^{-4}$  extrapolation of the radial profile provided by the whistler technique (limited to  $L < 4.3$ ) up to the DE 1 L shell ( $L = 4.6$ ) agrees with the satellite's measurement. At the 6.6 L shell, both satellites report similar figures: the density distribution along flux tubes does not appear to contain significant latitudinal or longitudinal irregularities.

4. Discussion

The observations reported above result from several physical processes at work in the outer plasmasphere. We will focus here on ionosphere-magnetosphere coupling, and discuss the evolution of the plasma characteristics along the magnetic field lines. The DE 1 orbit stays close to the same L shell in a rather large latitudinal range (Figure 1). However, one must emphasize that, according to the convection conditions, DE scans a large segment of plasma in longitude. Outside this range, the L values vary

rapidly and the satellite encounters different plasma regimes in crossing field-aligned boundaries. As stated above, the outermost L shell limiting a homogeneous plasmasphere did vary with time during the few days of our study. We shall discuss first the observations made in the expanded bulge, during near-equilibrium conditions, and then examine the dynamical refilling period.

4.1. Latitudinal Density Distribution in the Expanded Bulge

Considering the smoothness of the density profiles recorded by DE 1 inside the expanded bulge, it seems reasonable, using an appropriate scaling factor, to derive the density variations along a given field line from the measured densities along the satellite's orbit. We have applied this approach to the May 25 profiles, when GEOS 2 densities reach values similar to the DE 1 values on the 6.6 L-shell (Figure 6). We have normalized  $N_e$  values between minus and plus  $60^\circ$  latitude to values expected on the 4.54 shell at the same latitudes.

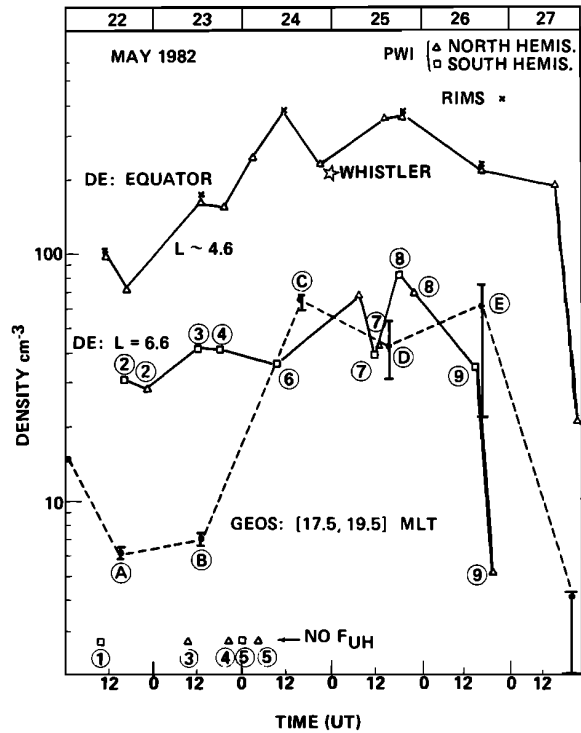


Fig. 6. Compared electron density data. DE 1 density data are plotted at the equator and at the GEOS 2 L shell. The circled numbers refer to the DE 1 profile numbers as indicated in Figure 5 and the circled letters to the GEOS 2 orbits as indicated in Figure 4. The times when PWI data were available, but no  $F_{UH}$  signature was observed at 6.6 L shell are indicated at the bottom of the figure. The whistler measurement (at 1800 MLT) corresponds to  $L = 4.6$ . The error bars in GEOS values (at 1830 MLT) cover the density variations observed in the (1730-1930) MLT range, where the DE values are taken.

The scaling factor used results from two hypotheses. The first one is to consider that the total electron content of the magnetic flux tubes covering the L range (4.3-7) swept by DE 1 in the  $\pm 60^\circ$  latitudinal range is a constant per unit magnetic flux. This hypothesis, sustained by experimental observations [Angerami and Carpenter, 1966], corresponds to a condition of the same influx of plasma from the ionosphere into a region of empty flux tubes. The rate of change of the number of plasmasphere electrons per unit magnetic flux at daytime is proportional to the upward flux of particles from the ionosphere, and to the cross-sectional area at the exobase. At nighttime, it is proportional to the total electron content [Chen and Wolf, 1972]. To a first approximation (a few percent), the variable cross-sectional area at the exobase is the same for the different flux tubes over the useful L range. We assume further that during the refilling period (a few days), the flux tubes stay in daytime for the same duration, and that they receive the same flux  $f_i$  at a given time. Finally, we consider that the measurement time (one DE 1 pass) is short versus the total duration of the refilling period.

Assuming the conditions for constant electron content per unit magnetic flux are fulfilled, a second hypothesis about the distribution of that content in the bulge, e.g. a constant density along field lines gives the required scaling factor. A comparison of the derived profile with the expected profile allows a justification a posteriori of our second hypothesis.

In the case of the simple hypothesis of a constant density along the field lines,  $N_e$  varies as  $L^{-4}$ , the inverse of the volume of a tube of unit magnetic flux (in the approximation of the dipole). Given that scaling factor, we have normalized the density profiles measured on May 25 to the 4.54 L shell (Figure 7). Both profiles show only negligible variations over a large latitudinal range ( $\pm 35^\circ$ ). The first one (1120-1600 UT) shows a density gradient near  $40^\circ$  magnetic latitude in both hemispheres, which we interpret as being a plasmopause gradient, since the GEOS 2 equatorial density agrees with the value measured on the flanks of the gradients by DE 1. During the next pass, no evolution is observed in the measured equatorial densities. The plasmopause boundary is located at higher L shells, at least in the southern hemisphere.

The densities measured at the equator ( $N_e \approx 350 \text{ cm}^{-3}$ ) approach the maximum level ( $N_e \approx 450 \text{ cm}^{-3}$ ) measured at the same L value during a one-month campaign in summer using the whistler technique [Park et al., 1978]. The maximum value observed in the outer plasmasphere, which we will qualify hereafter as a "plasmasphere density level," does not imply necessarily a physical process that chokes off the ionospheric flow as higher electron contents are reached. It may simply correspond to the maximum duration of very quiet magnetic conditions, of the order of a few days, during which the refilling process may operate efficiently. In the case under study, the two May 25 profiles observed on DE 1, several hours apart, show the same density level, close to values reached already on May 24 (Figure 6), and close to the "plasmasphere" level. They indicate that the flux tubes have reached a state

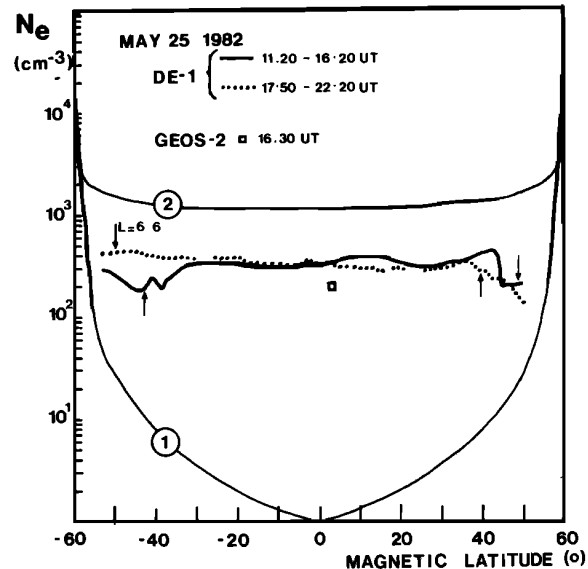


Fig. 7. Latitudinal electron density profiles along a field line. Experimental data from DE 1 have been normalized to the 4.54 L shell. The latitudes at which the satellite crosses the 6.6 L shell are indicated by arrows. The value measured by GEOS 2 the same day at (1842) MLT is also reported after normalization to the same L shell. Curves 1 and 2, refer to theoretical profiles for the  $L = 4.54$  field line, respectively in a collisionless model (1), and a diffusive equilibrium model (2). The boundary conditions for the two cases are taken from model 1 [Lemaire and Scherer, 1974].

of quasi-equilibrium, where plasma losses may balance the ionospheric input under specific conditions. For instance, limited plasma losses due to plasma interchange motion are expected when the magnetic activity is low and when plasma structures are present in the outer plasmasphere [Lemaire and Kowalkowski, 1981], which is the case for the period studied.

For the sake of comparison, we have plotted in Figure 7 two theoretical latitudinal profiles which describe the outer plasmasphere region. Profile 1 is reproduced from Lemaire and Scherer [1974]. It gives the electron density along the field line intersecting the exobase (located at 870 km altitude) at  $60^\circ$  dip latitude (for the 4.54 L shell), in a nonrotating collisionless model. The two main ion species ( $O^+$  and  $H^+$ ) are taken into account, and exobase densities and temperatures are taken from experimental values measured in this region (with  $N_e = 2.06 \cdot 10^4 \text{ cm}^{-3}$ ,  $T_e = 2500^\circ\text{K}$ ,  $N_{H^+}/N_{O^+} = 0.03$ ). At low latitudes, this model yields much lower densities than those measured, due to the fact that all trapped particle orbits are considered as unoccupied.

The distribution in a diffusive equilibrium situation which takes an opposite point of view (the hydrodynamic approach, where collisions dominate) is calculated after Angerami and Thomas [1964], also for the  $L = 4.54$  field line (profile 2). We have used the same boundary conditions used for profile 1. This time, the calculated

densities are higher by roughly a factor of 3 from the measured values, but the shape of the model fits the data in the equatorial region. It is interesting to note that in an independent study, dealing with VLF propagation paths in the same region of the magnetosphere for the same day (May 25, 1982), Rastani et al. [1985] have concluded that the diffusive equilibrium model provides good agreement with measurements over a wide range of magnetic latitudes (50°S-25°N).

Other plasmasphere models relevant to the 4-5 L range have been examined. Most of them yield a density distribution with a significant minimum in the equatorial region. This is the case for the dynamical diffusive model of Mayr et al. [1970], which assumes a constant loss of plasma at the equator, as well as for the refined equilibrium models of Chiu et al. [1979] and of Li et al. [1983] which allow for magnetic field divergence and temperature variation along the field line. On the contrary, models restricted to the inner plasmasphere account for almost constant density values along field tubes in the equatorial region [Young et al., 1980].

The fact that at least in the observable range  $\pm 40^\circ$  the observed shape of the latitudinal density distribution fits the diffusive equilibrium model, or models pertaining to the inner plasmasphere, supports the idea that a certain pressure equilibrium along the field line has been reached. The diffusion of ionospheric particles, through thermalization or other mechanisms, has been efficient, and trapped particle orbits are occupied. However, the discrepancy between the observed density level and values provided by the simple diffusive equilibrium model is important: in fact, electron densities above  $800 \text{ cm}^{-3}$  at  $L \approx 4.5$  are almost never observed. In order to check the boundary conditions used in the model, we have examined the electron densities and temperatures measured in the ionosphere (between 500 and 700 km altitude) by the DE 2 satellite on May 25, in the same MLT and L range (L. Brace, private communication, 1984). On the average, they agree with the values chosen. However, they vary with time, and the northern (sunlit) hemisphere is denser ( $N_e \approx 10^5 \text{ cm}^{-3}$ ) than the southern one ( $N_e \approx 10^4 \text{ cm}^{-3}$ ). The use of a simple model is consequently limited. We consider as satisfactory the fact that a closer fit from the model to the data leads to implications regarding the lower boundary (a factor of 3 in the density level, if the other assumptions are correct) that are not unreasonable.

Finally, we would like to comment on specific physical processes which can explain the relatively low densities observed independently of the limitations in the model used. One of them is the presence of cross-L drifts of plasma, through the convection phenomena. The comparison of GEOS 2 and DE 1 data (section 3) has shown that, due to the dynamics of the convection, the May 25 profiles observed on both satellites likely originated in a region which was deeper within the plasmasphere at an earlier time. Actually, an increase of magnetic activity is known to be correlated with sunward and outward motions of the plasmaspheric particles in the afternoon sector [Carpenter and Seely, 1976; Carpenter et al., 1979; Baumjohann et al., 1985].

When the corresponding plasma clouds are moved from low to high L shells, most particles remain distributed with constant density along the field line. In fact, the low pressure formed in the tube tends to suck more particles from the ionosphere [Marubashi, 1979] toward high altitudes. However, as the tube volume increases, the density decreases as  $L^{-4}$ , i.e., has a more rapid variation with L than in the case of a steady state diffusive equilibrium everywhere. Such a scenario would end up with an experimental density profile showing a reduced level as compared to what is expected for diffusive equilibrium in a field tube of constant volume. Moreover, as stated above, the probability of plasma losses above  $L = 4$ , combined with saturation effects when the plasma is compressed to low L shells, is high enough to prevent the steady state level from ever being reached in practice in this region.

#### 4.2. Convection Scenario During the Replenishment Phase (May 22-23)

In order to discuss the significance of the plasma fluctuations observed on May 22-23, it is important to have a good idea of what could be attributed to field-aligned irregularities expected from variable geophysical conditions rather than to latitudinal effects. The plasmopause boundary can depart from a dipolar magnetic-shell shape, through a magnetic field deformation. In addition, the plasmopause can display azimuthal density irregularities. A north-south asymmetry of field lines above  $L = 5$  is present in realistic magnetic field models such as the Mead and Fairfield model, but it is negligible near 1800 MLT [Fairfield and Mead, 1975]. The measured components of the interplanetary magnetic field (IMF) during the days May 22-23 (J. Berchem, private communication, 1984), when added to the Earth dipole field [Lyons, 1985], do not produce significant perturbations of the magnetic field in the internal magnetosphere. On the contrary, the presence of irregularities in the shape of the plasmopause, observed as variations of the equatorial plasmasphere radius or of equatorial densities versus longitude or local time, is a known and common phenomenon [Carpenter, 1983; Higel and Wu Lei, 1984; Décréau, 1983]. Carpenter [1983] notes that one major source for them appears to be cross-L drifts associated with substorms in the postmidnight sector.

The analysis of whistler data recorded at the Siple ground station for several periods of May 22 and early May 23 shows clear evidence of longitudinal density gradients in the 4-5 L range. One of them, with an amplitude of a factor of 2, is seen at about 1830 MLT near 2330 UT, May 22. This type of irregularity can account for the density fluctuations reported in the profile of May 22, 1650 UT (Figure 5). It is consistent with the variability of the convection electric field measured on GEOS 2 at the same time. Moreover, the localized increase of magnetic activity observed in the first hours of May 23 is clearly associated with a substantial enhancement of the convection electric field and the subsequent creation of important azimuthal plasma depletions. We have indications of this scenario



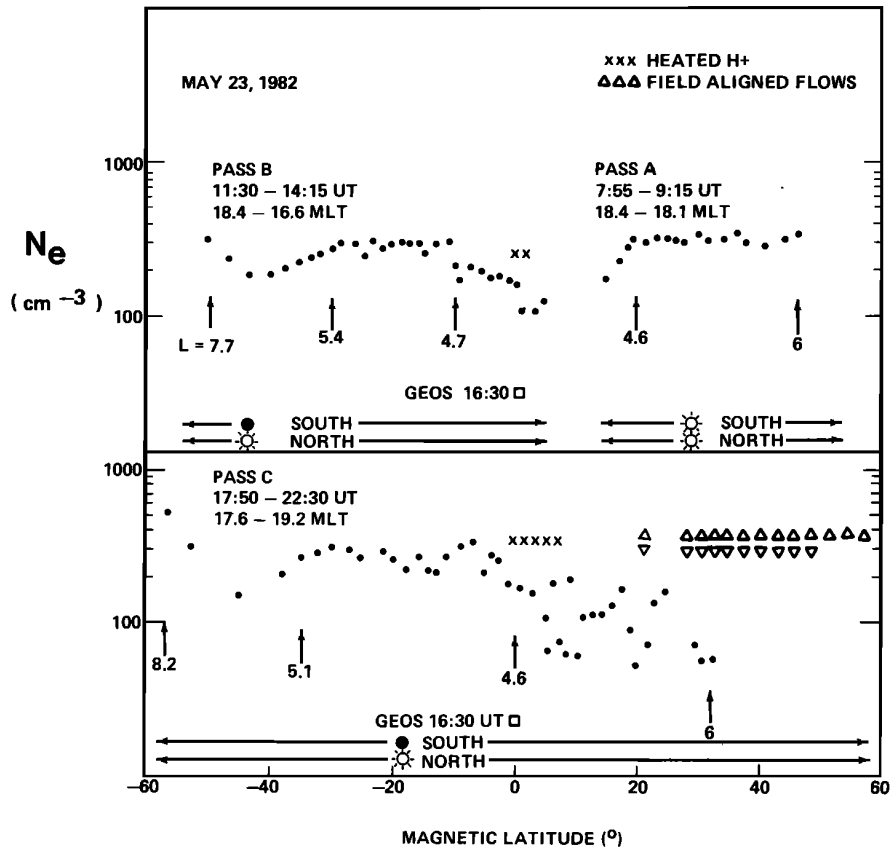


Fig. 8. Latitudinal electron density profiles normalized at  $L = 4.54$  during the refilling period. The GEOS value plotted is measured the same day. The open and solid sun symbols indicate if the ionosphere at each foot of the field lines crossed by DE 1 is respectively sunlit or in shadow.

from two data sources. The GEOS 2 density profile of orbit A, Figure 4, reports a sharp gradient crossed between 0000 and 0100 UT. In addition, just prior to 0300 UT, the low-altitude DE 2 spacecraft, located near 1800 MLT, measures a poleward convection electric field which corresponds to sunward drifts, down to middle invariant latitudes (N. Maynard, private communication, 1984). Several observations on May 23—the apparent hemispheric asymmetry in the DE 1 profile 4 (Figure 5), and discrepancies between GEOS 2 and DE 1 measurements (Figure 6)—could be explained by the relative motion of field-aligned irregularities with respect to DE 1.

#### 4.3. Latitudinal Effects on Plasma Characteristics During Plasmasphere Refilling

Striking results have been obtained from the analysis of the density profiles recorded during the recovery phase of May 22-23, in terms of possible latitudinal effects. The data show two main characteristics that we will comment upon in turn: (1) the presence of plasma structures, already pointed out above, and (2) the evidence of field-aligned flows, which are illustrated further by complementary data, taken a few days later.

Latitudinal density profiles from the three

passes of May 23 are presented in Figure 8. As in Figure 7, the values plotted are electron densities normalized to the  $L = 4.54$  field line, according to an  $L^{-4}$  volume variation of the magnetic flux tubes. In contrast to what was accomplished in dealing with the smooth profiles of the expanded bulge (section 4.1), we do not expect here to obtain the shape of the density distribution along a given field line. The normalization of the measurements to a given volume of field tube still helps to point out departures from the simple distribution of particles with constant flux tube content and constant density. The upper panel of Figure 8 refers to two successive profiles (A and B) measured respectively in the northern and southern hemispheres. The profile of pass C (lower panel) covers the two hemispheres.

A first outcome of these graphs is that there is no indication of density enhancement in the vicinity of the equator, just as there was none in the case of the expanded bulge region. Actually, the analysis of the complete set of electron density profiles obtained on DE 1 and GEOS 2 in the period May-June 1982 confirms this result. Different plasma regions show up in the three profiles of Figure 8. In limited parts of the profiles ( $\approx 25^\circ$  to  $50^\circ$  latitude, pass A;  $\approx 30^\circ$  to  $0^\circ$ , pass B and pass C) the density stays roughly constant, close to the typical

plasmasphere values of the expanded bulge. The presence of higher densities at the beginning of passes B and C (a byproduct of the  $L^{-4}$  normalization) shows that the effect of increasing density with decreasing altitude (cf. theoretical profiles in Figure 7) overcomes the effect of decreasing total content with  $L$ . The other structures observed—a plasma depression at the equator, associated here with an increased proton temperature, as well as large density fluctuations in the northern part of pass C—are interpreted as being related to azimuthal density gradients, as we observe no similar latitudinal patterns from one pass to another.

On pass C, the RIMS instrument shows clear evidence of interhemispheric plasma transport in the northern part of the orbit (Figure 8): in between the plasma clouds encountered, which are formed likely by plasmopause irregularities, the satellite penetrates the refilling region, characterized by low densities and field-aligned flows. The signature of the latter feature is shown in Plate 1a, which displays a spin-time spectrogram of the count rates measured by the radial head of the instrument. (Plate 1 is shown here in black and white. The color version can be found in the separate color section in this issue.) The radial head points perpendicular to the spin axis, with an angular acceptance of  $\pm 10^\circ$  in the pitch angle plane, which is the plane of the orbit, and of  $\pm 55^\circ$  in the plane containing the spin axis. The time is plotted along the horizontal axis of the spectrogram, and the spin angle, given with respect to the spacecraft ram direction, along the vertical axis. The white lines refer to minimum angles ( $\sim 0^\circ$ ) between the instrument's direction and the magnetic field: north and south are indicated respectively by the dashed and the dotted lines. As mentioned above (section 2) the proton angular distribution is not available for this pass, but the helium distribution is a good indicator of the plasma regime. An isotropic Maxwellian plasma shows a spin angle response peaking in the ram direction, as seen on most of the southern part of the orbit. In the case of a field-aligned distribution (at  $\sim 2055$  UT and after 2130 UT) the spin angle response peaks along the magnetic field, in one or both directions, with a slight shift due to the ram effect.

Field-aligned angular distributions are not restricted to the refilling region. On DE 1, they are commonly observed in the auroral region, as well as over the polar cap [Chappell et al., 1982a; Moore et al., 1985; Waite et al., 1985]. On ISEE 1, the bidirectional field-aligned distribution of warm ions ( $\sim 10$  eV) is a permanent feature seen outside the plasmasphere [Nagai et al., 1984]. Whereas in the polar cap both thermal and suprathermal flows are observed, the upward acceleration of ions is a dominant process in the auroral region, and leads to measured characteristic energies of tens of electron volts [Chappell, 1983]. For the event studied, the equatorward boundary of the diffuse aurora as measured on the DE 2 satellite (D. Winningham, private communication, 1984) is located at  $L$  shells of 8.5 or higher, which confirms that DE 1 and GEOS 2 are in a refilling region located equatorward of the field tubes

where auroral acceleration takes place, at least before 2220 UT for the northern part of the DE 1 pass C. It is important to mention that the RIMS instrument aperture was biased 8 volts negative relative to the spacecraft, during pass C. A negative bias is aimed to collect the particles of low temperature in spite of a positive spacecraft potential resulting from the low density environment. The observed spin angle variations, provided they correspond to a drifting thermal and isotropic population, may be used to characterize further the particle distribution. We have analyzed the spin angle curves from 2135 to 2145 UT. The magnitude of the  $\text{He}^+$  upward velocity along the field line, deduced from the position of the main peak, stays around  $2 \text{ km s}^{-1}$  (M. Chandler, private communication, 1984). The width of the peak, and an estimate of the potential of the satellite (+ 4 volts), lead through a best fit analysis using the thin sheath model [Comfort et al., 1982] to an estimated temperature of  $2000^\circ \text{ K}$ , which corresponds to a slightly supersonic flow. However, a subsonic flow of a primarily collimated warmer distribution would lead to the same observations, which prevents us from arriving at any definite conclusion on the Mach number of the flow.

In any event, the observation of interhemispheric transport of possibly cold plasma in the refilling region brings a new insight into the physics of this region. Field-aligned flows were not observed in a DE 1 study of the plasmasphere formation at low altitude ( $R \approx 3 R$ ) presented by Horwitz et al. [1984]. However, the authors state that the observation of such distributions may have been obscured in their study by a positive spacecraft potential. In their detailed analysis of ion measurements by the RIMS instrument during one pass of DE 1, Sojka et al. [1983] report about thermal field-aligned ions observed above 3 earth radii geocentric distance, in the outer plasmasphere ( $3.8 < L < 4.7$ ) at 0900 LT. In this case DE 1 had cut the refilling field tubes approximately halfway between the ionosphere and the equator. In order to confirm our observations, we have examined RIMS data under the relevant conditions (in the refilling region and for negative aperture bias) in the period May-July 1982, and found several clear cases of interhemispheric flows, for most cases covering the equatorial region. One example is shown in the lower panels of Plate 1. For this event (June 4, 1982) the experimental conditions are similar to those of May 23, pass C: the southern foot of the field lines is in darkness and the northern foot sunlit; a decrease of magnetic activity, after moderate conditions, occurs during several hours preceding the pass; GEOS 2 measurements report a constant density of approximately  $7 \text{ cm}^{-3}$  in the dusk sector; and the equatorward boundary of the diffuse aurora as measured on DE 2 is located at high  $L$  shells ( $> 8$ ). In the case of the June 4 pass, the electron density has been measured over most of the latitudinal range. The value reported at the equator is consistent with the GEOS 2 measurement ( $7 \text{ cm}^{-3}$  after a  $L^{-4}$  normalization), from which we conclude that, contrary to the May 23 pass C, DE 1 stays outside the plasmasphere (like GEOS 2) for the complete

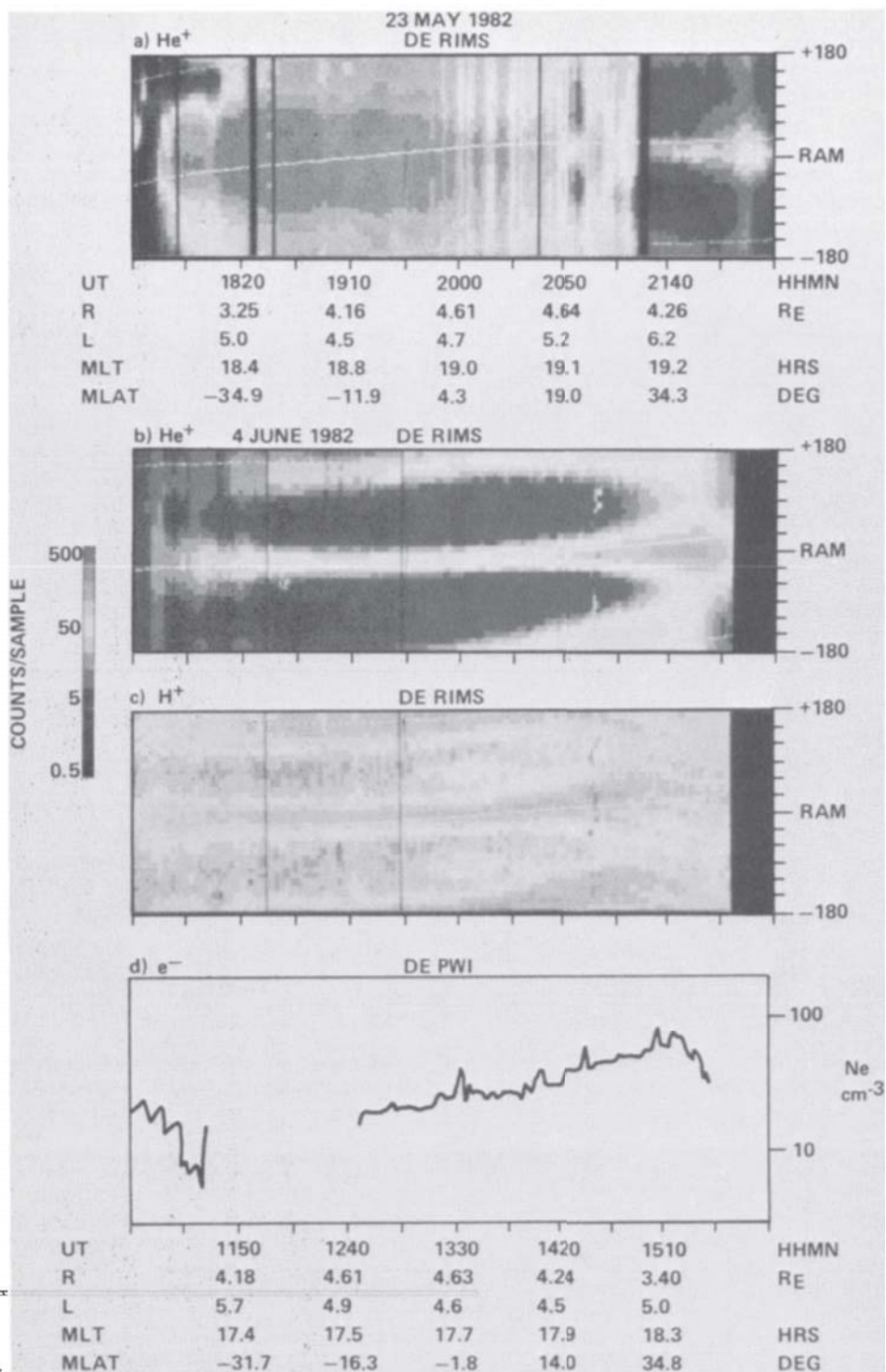


Plate 1. Spin angle-time spectrograms for (a) He<sup>+</sup> during 1730-2230 UT, May 23, 1982, (b and c) He<sup>+</sup> and H<sup>+</sup> during 1100-1600 UT, June 4, 1982. (d) The electron density variations for the second time period. The color version and a complete description of this figure can be found in the separate color section in this issue.

orbit. The observations taken on this orbit are consequently adapted to a discussion on the evolution of the plasma characteristics versus latitude in the refilling region.

We do notice from Plates 1b-1d latitudinal effects inside the flux tubes which are in the process of being replenished by the ionosphere. In this case, we have not used any density normalization versus the field tubes' volume, as the L variation over a large part of the orbit (from 1240 to 1510 UT) is reduced to the range 4.5 to 5.0, with correspond to limited volume variations and do not prevent qualitative conclusions. It is striking to note that, in opposition to the density distribution observed along the field line in the expanded bulge, there is a continuous increase of density with latitude in the northern hemisphere (Plate 1d), although the L value is increasing: the altitude effect seems to be important, in agreement with the collisionless model where trapped particle orbits are unoccupied (Figure 7). The Kp evolution for June 4, which indicates a low magnetic activity for six to nine hours before the pass, as well as the magnitude of the equatorial density, requires a refilling time of the flux tubes of 6 to 12 hours. The model of Banks et al. [1971], relevant to symmetric boundary conditions, predicts that after 10 hours of refilling, the shock front formed at the magnetic equator, with a density discontinuity of about a factor of four, has traveled down the field lines to about 45° latitude, so that all measurements in the ± 40° latitude range are taken inside the equatorial hot postshock region. This model, as well as the model of Schulz and Koons [1972] with no initial confining of plasma about the equator, emphasizes the thermalization mechanisms which affect the supersonic flows counterstreaming from conjugate ionospheres in the early stage of the replenishment phase. However, contrary to model predictions, the major part of the observed distribution in this latitude range stays field aligned. Actually, the real conditions governing the starting phase of the replenishment process (nonzero pressure in the field tubes, nonsymmetric boundary conditions at the conjugate ionospheres) may lead to a refilling mechanism where the interhemispheric flows reach a subsonic regime rapidly and where critical conditions for particle diffusion are not met. The other observations of counterstreaming flows in the equatorial part of the refilling region made on DE 1 by the RIMS instrument show similar patterns: the density distribution tends to fall off more steeply near the equator than diffusive equilibrium.

Another interesting feature, which shows up both in the May 23 pass C (near 2210 UT) and in the June 4 pass (near 1520 UT), is the crossing of a region of moderate density with a scattered angular distribution (at  $R \approx 3 R_E$ ), before the satellite enters a region where the ions are seen as coming only from the closest ionosphere. Sojka et al. [1983] note that one explanation of the disappearance of one of the counterstreaming beams is the existence of a trapping or thermalization of the beam at an altitude higher than the satellite. If so, it may not necessarily be at the equator, but could result in mirror points located at middle latitudes, and explain

the observed accumulation of plasma. Further studies are necessary to understand the implications of the apparent density maximum observed along the orbit, as it could as well be simply related to plasma conditions varying in the field tubes of increasing L values crossed successively by DE 1.

## 5. Summary

We have studied the morphology and dynamics of the plasmaspheric bulge through the correlation of different data sources, mainly the DE 1 and GEOS 2 spacecraft traveling in two perpendicular planes. A first outcome of this study is that the bulge is a dynamic region, where no reasonable interpretation of the observed density distribution can be achieved without taking into account the mechanism of magnetospheric convection. Since the main purpose of this study is to get a better idea of the latitudinal extension of the bulge through direct in situ measurements, we have presented the DE 1 data in terms of density profiles along field lines.

Different plasma regimes are observed throughout the period studied. After three days of quiet activity disrupted by an isolated substorm (May 22-24), the Kp indices progressively increase up to values of 6 (May 26). The beginning of the sequence is marked by the replenishment of depleted flux tubes from the ionospheric source. GEOS 2 stays outside the plasmapause boundary, measuring densities ( $5\text{-}10 \text{ cm}^{-3}$ ) characteristic of a first step (less than 24 hours) of replenishment during two successive days, as an isolated substorm occurred in between. DE 1 reported irregular plasma characteristics, showing the existence, in the outer plasmasphere, of structures of higher densities which may be azimuthal and possibly drifting. It is known [Park and Carpenter, 1970; Chen and Wolf, 1972; Morgan and Maynard, 1976; Grebowsky and Chen, 1976] that the plasmapause boundary is shaped by long- and short-term variations of the convection pattern, so that this mechanism could explain most of the morphological features reported in our data set, in particular as concerns the cold thermalized population. On the other hand, the unique ability of the RIMS instrument to measure the angular distribution of low energy ions gives direct evidence of interhemispheric flows during the refilling period in the low density region. This signature is associated with a smooth increase of the density versus latitude. The observed characteristics of the plasma regime in the refilling region, after several hours of replenishment, are not consistent with the features expected under the hypothesis of empty flux tubes and symmetric ionospheric conditions. Rather, experimental data indicate an accumulation of warm plasma at about 3 earth radii and 40° latitude, in one or both hemispheres, and a double field-aligned regime in the equatorial region.

The second part of the period studied is characterized by "high" ( $50 \text{ cm}^{-3}$ ), rather stable densities measured on the 6.6 L shell: the body of the plasmasphere has expanded radially out to the geostationary orbit. Azimuthal irregularities observed (from May 25 on) during the "expanded

bulge period" are likely triggered by the onset of substorms. The latitudinal density profiles measured on May 25 (as on the preceding day) below  $L = 6$  are nevertheless smooth, showing a striking constant density over a large range of latitudes ( $\pm 40^\circ$ ). We interpret this last feature as due to the fact that the bulge is the expansion, via convective motion, of plasma tubes formerly part of an inner plasmasphere in diffusive equilibrium with the ionosphere. The last day of our study (May 26) is marked by sunward drifts which result in the depletion of field tubes.

Coming back to our first concern of the latitudinal extension of the dusk bulge of the plasmasphere, we can conclude from our analysis that, if there is a lack of connection between the bulge and the underlying ionosphere, this occurs outside the  $\pm 40^\circ$  magnetic latitude range. In the entire period May-June 1982, we have no cases of plasmaspheric densities at GEOS 2 latitude associated with low densities at DE 1 latitude on the same  $L$  shell. Moreover, no density enhancements restricted to the equatorial region, even in the cases of proton heating or during the replenishment process. However, since DE 1 sweeps a range of  $L$  shells and longitudes along its orbit, our data set is by nature unable to reveal the latitudinal distribution of density down to the scale of a given magnetic field tube with homogeneous cross-section plasma characteristics. More systematic large-scale studies, under different convection conditions, should help to resolve the uncertainty between azimuthal, radial, and latitudinal irregularities and should be most useful for the study of ionosphere-magnetosphere coupling, plasmasphere refilling, and plasma equilibrium along field lines.

**Acknowledgments.** The authors are indebted to the engineering and science staff of the University of Texas at Dallas and to the RIMS team at Marshall Space Flight Center (MSFC). We are grateful to the programming staff of the Intergraph and Boeing Corporations for assistance with the data reduction software and to the MSFC/SCAN network for support of the graphics analysis. Significant data analysis contributions were also made by Teresa Felch. We thank A. Pedersen, for providing electric field data on GEOS 2, D. Weimer for analysis of electric field data on DE 1, J. Etcheto and J. G. Trotignon for providing electron densities on ISEE 1, as well as the S300 experimenters for access to wave data on GEOS 2 and D. Gurnett for access to wave data on DE 1. Two of us (R.H.C and R.C.O) have been partially supported in this work by NSF grant ATM-8300426 and NASA contract NA58-33982 with the University of Alabama in Huntsville. Support for P. M. E. Décréau came from on National Research Council Resident Research Associateship at NASA/MSFC.

The Editor thanks J. J. Sojka and D. Winningham for their assistance in evaluating this paper.

#### References

- Angerami, J. J., and D. L. Carpenter, Whistler studies of the plasmopause in the magnetosphere, 2, Equatorial density and total tube electron content near the knee in magnetospheric ionization, *J. Geophys. Res.*, **71**, 711, 1966.
- Angerami, J. J., and J. O. Thomas, Studies of planetary atmospheres, 1, the distribution of electrons and ions in the earth's exosphere, *J. Geophys. Res.*, **69**, 4537, 1964.
- Banks, P. M., A. F. Nagy, and W. I. Axford, Dynamical behavior of thermal protons in the mid-latitude ionosphere and magnetosphere, *Planet. Space Sci.*, **19**, 1053, 1971.
- Baumjohann, W., G. Haerendel, and F. Melzner, Magnetospheric convection observed between 0600 and 2100 LT: Variations with Kp, *J. Geophys. Res.*, **90**, 393, 1985.
- Brace, L. H., and R. F. Theis, The behavior of the plasmopause at mid-latitudes: Isis I Langmuir probe measurements, *J. Geophys. Res.*, **79**, 1871, 1974.
- Carpenter, D. L., Some aspects of plasmopause probing by whistlers, *Radio Sci.*, **18**, 917, 1983.
- Carpenter, D. L., and N. T. Seely, Cross-L plasma drifts in the outer plasmasphere: Quiet time patterns and some substorm effects, *J. Geophys. Res.*, **81**, 2728, 1976.
- Carpenter, D. L., C. G. Park, and T. R. Miller, A model of substorm electric fields in the plasmasphere based on whistler data, *J. Geophys. Res.*, **84**, 6559, 1979.
- Chappell, C. R., Initial observations of thermal plasma composition and energetics from Dynamics Explorer 1, *Geophys. Res. Lett.*, **9**, 929, 1982.
- Chappell, C. R., Cold plasma distribution above a few thousand kilometers at high latitudes, in *High-Latitude Space Plasma Physics*, edited by B. Hultqvist and T. Hagfors, p. 251, Plenum, New York, 1983.
- Chappell, C. R., J. L. Green, J. F. E. Johnson, and J. H. Waite, Jr., Pitch angle variations in magnetospheric thermal plasma-Initial observations from Dynamics Explorer-1, *Geophys. Res. Lett.*, **9**, 933, 1982a.
- Chappell, C. R., S. A. Fields, C. R. Baugher, J. H. Hoffman, W. B. Hanson, W. W. Wright, and H. D. Hammack, The retarding ion mass spectrometer on Dynamics Explorer-A, *Space Sci. Instrum.*, **5**, 477, 1982b.
- Chen, A. J., and R. A. Wolf, Effects on the plasmasphere of a time-varying convection electric field, *Planet. Space Sci.*, **20**, 483, 1972.
- Chiu, Y. T., J. G. Luhmann, B. K. Ching, and D. J. BOUCHER, Jr., An equilibrium model of plasmaspheric composition and density, *J. Geophys. Res.*, **84**, 909, 1979.
- Comfort, R. H., C. R. Baugher, and C. R. Chappell, Use of the thin sheath approximation for obtaining ion temperatures from the ISEE 1 limited aperture RPA, *J. Geophys. Res.*, **87**, 5109, 1982.
- Comfort, R. H., J. H. Waite, Jr., and C. R. Chappell, Thermal ion temperatures from the retarding ion mass spectrometer on DE 1, *J. Geophys. Res.*, **90**, 3475, 1985.
- Corcuff, Y., and P. Corcuff, Structure et dynamique de la plasmopause-plasmasphère les 6 et 14 juillet 1977: Etude à l'aide des données de sifflements recus au sol et de données des

Angerami, J. J., and D. L. Carpenter, Whistler studies of the plasmopause in the

- satellites ISIS et GEOS, Ann. Geophys., 38, 1, 1982.
- Décrou, P. M. E., Fonctionnement d'une sonde quadripolaire sur satellite magnétosphérique (expérience GEOS) - Contribution à l'étude du comportement du plasma froid au voisinage de la plasmopause équatoriale, state doctorate thesis, Univ. of Orléans, France, 1983.
- Décrou, P. M. E., C. Béghin, and M. Parrot, Electron density and temperature as measured by the mutual impedance experiment onboard GEOS1, Space Sci. Rev., 22, 581, 1978a.
- Décrou, P. M. E., J. Etcheto, K. Knott, A. Pedersen, G. L. Wrenn, and D.T. Young, Multi-experiment determination of plasma density and temperature, Space Sci. Rev., 22, 633, 1978b.
- Etcheto, J., and J. J. Bloch, Plasma density measurements from the GEOS 1 relaxation sounder, Space Sci. Rev., 22, 597, 1978.
- Fairfield, D. H., and G. D. Mead, Magnetospheric mapping with quantitative geomagnetic field model, J. Geophys. Res., 80, 535, 1975.
- Grebowsky, J. M., and A. J. Chen, Effects on the plasmasphere of irregular electric fields, Planet. Space Sci., 24, 689, 1976.
- Harvey, C. C., J. Etcheto, Y. De Javel, R. Manning, and M. Petit, The ISEE electron density experiment, IEEE Trans. Geosci. Electron., GE-16, 253, 1978.
- Higel, B., and Wu Lei, Electron density and plasmopause characteristics at 6.6 R : A statistical study of the GEOS 2 relaxation sounder data", J. Geophys. Res., 89, 1583, 1984.
- Horwitz, J. L., Major questions on the interchange of thermal plasmas between the ionosphere and magnetosphere, J. Atmos. Terr. Phys., 45, 765, 1983.
- Horwitz, J. L., C. R. Baugher, C. R. Chappell, E. G. Shelley, and D. T. Young, Pancake pitch-angle distributions in warm ions observed with ISEE 1, J. Geophys. Res., 86, 3311, 1981.
- Horwitz, J. L., R. H. Comfort, and C. R. Chappell, Thermal ion composition measurements of the formation of the new outer plasmasphere and double plasmopause during storm recovery phase, Geophys. Res. Lett., 11, 701, 1984.
- Lemaire, J., and L. Kowalkowski, The role of plasma interchange motion for the formation of a plasmopause, Planet. Space Sci., 29, 469, 1981.
- Lemaire, J., and M. Scherer, Exospheric models of the topside ionosphere, Space Sci. Rev., 15, 591, 1974.
- Li, W., J. J. Sojka, and W. J. Raitt, A study of plasmaspheric density distributions for diffusive equilibrium conditions, Planet Space Sci., 31, 1315, 1983.
- Lyons, L., A simple model for polar cap convection patterns and generation of  $\theta$ -auroras, J. Geophys. Res., 90, 1561, 1985.
- Marubashi, K., Effects of convection electric field on the thermal plasma flow between the ionosphere and the protonosphere, Planet. Space Sci., 27, 603, 1979.
- Mayr, H. G., J. M. Grebowsky, and H. A. Taylor, Jr., Study of the thermal plasma on closed field lines outside the plasmasphere, Planet. Space Sci., 18, 1123, 1970.
- Moore, T. E., C. R. Chappell, M. Lockwood, and J. H. Waite, Jr., Suprathermal ion signatures of auroral acceleration processes, J. Geophys. Res., 90, 1611, 1985.
- Morgan, M. G., and N. C. Maynard, Evidence of plasmaspheric structure through comparisons of ground-based whistler data and Explorer 45 plasmopause data, J. Geophys. Res., 81, 3992, 1976.
- Nagai, T., J. H. Waite, Jr., J. L. Green, C. R. Chappell, R. C. Olsen and R. H. Comfort, First measurements of supersonic polar wind in the polar magnetosphere, Geophys. Res. Lett., 11, 669, 1984.
- Olsen, R. C., Equatorially trapped plasma populations, J. Geophys. Res., 86, 11235, 1981.
- Olsen, R. C., The hidden ion population of the magnetosphere, J. Geophys. Res., 87, 3481, 1982.
- Olsen, R. C., D. L. Gallagher, C. R. Chappell, J. L. Green and S. D. Shawhan, A potential control method for thermal plasma measurements on the DE1 spacecraft, paper presented at 17th ESLAB Symposium on Spacecraft/Plasma Interactions and Their Influence on Field and Particle Movements, Noordwijk, The Netherlands, 13-16 sept. (ESA SP-198, publ. december 1983).
- Park, C. G., Whistler observations of the interchange of ionization between the ionosphere and the protonosphere, J. Geophys. Res., 75, 4249, 1970.
- Park, C. G., and D. L. Carpenter, Whistler evidence of large-scale electron-density irregularities in the plasmasphere, J. Geophys. Res., 75, 3825, 1970.
- Pedersen, A., R. Grard, K. Knott, D. Jones, A. Confalone and U. V. Fehleson, Measurements of quasi-static electric fields between 3 and 7 earth radii on GEOS-1, Space Sci. Rev., 22, 333, 1978.
- Rastani, K., U. S. Inan, and R. A. Helliwell, DE 1 observations of Siple transmitter signals and associated sidebands, J. Geophys. Res., 90, 4128, 1985.
- Reasoner, D. L., P. D. Craven, and C. R. Chappell, Characteristics of low-energy plasma in the plasmasphere and plasma trough, J. Geophys. Res., 88, 7913, 1983.
- Schulz, M., and H. C. Koons, Thermalization of colliding ion streams beyond the plasmopause, J. Geophys. Res., 77, 248, 1972.
- Shawhan, S. D., D. A. Gurnett, D. L. Odem, R. A. Helliwell, and C. G. Park, The plasma wave and quasi-static electric field instrument (PWI) for Dynamics Explorer-A, Space Sci. Instrum., 5, 535, 1981.
- Sojka, J. J., R. W. Schunk, J. F. E., Johnson, J. H. Waite, Jr., and C. R. Chappell, Characteristics of thermal and suprathermal ions associated with the dayside plasma trough as measured by the Dynamics Explorer retarding ion mass spectrometer, J. Geophys. Res., 88, 7895, 1983.
- S300 Experimenters, Measurements of electric and magnetic wave fields and cold plasma parameters onboard GEOS1-Preliminary results, Planet. Space Sci., 27, 317, 1979.

- Titheridge, J. E., Plasmopause effects in the topside ionosphere, J. Geophys. Res., 81, 3227, 1976.
- Waite, J. H., Jr., T. Nagai, J. F. E. Johnson, C. R. Chappell, J. J. Burch, T. L. Killeen, P. B. Hays, G. R. Carignan, W. K. Peterson, and G. L. Shelley, Escape of suprathermal  $O^+$  ions in the polar cap, J. Geophys. Res., 90, 1619, 1985.
- Wrenn, G. L., J. J. Sojka, and J. F. E. Johnson, Thermal protons in the morning magnetosphere: plasmopause, Planet Space Sci., 32, 351, 1984.
- Young, E. R., D. G. Torr, P. Richards, and A. F. Nagy, A computer simulation of the midlatitude plasmasphere and ionosphere, Planet. Space Sci., 28, 881, 1980.
- 
- D. Carpenter, Space, Telecommunications and Radioscience Laboratory, Stanford University, Stanford, CA 94305.
- C. R. Chappell, J. Green, and J. H. Waite, Jr., Space Science Laboratory, NASA Marshall Space Flight Center, Huntsville, AL 35812.
- R. H. Comfort and R. C. Olsen, Department of Physics, University of Alabama in Huntsville, AL 35899.
- P. M. E. Décréau, Laboratoire de Physique et Chimie de l'Environnement, 3A, Avenue de la Recherche Scientifique, 45071 Orléans Cédex 2, France.

(Received July 11, 1985;  
accepted September 16, 1985.)